ISSN 2689-8268 | Volume 5

American Journal of Surgery and Clinical Case Reports

Research Article Open Access

H2 Generation via CuS/C3N4 Nanocatalyst under Solar Light from the Municipale Wastewaters

Sponza DT*

Department of Environmental Engineering, Dokuz Eylül University, Engineering Faculty, Turkey

***Corresponding author:**

Delia Teresa Sponza,
Department of Environmental Engineering, Dokuz Eylül University, Engineering Faculty, Buca İzmir Turkey, E-mail: delya.sponza@deu.edu.tr

Received: 11 Aug 2022
Accepted: 18 Aug 2022
Published: 25 Aug 2022
J Short Name: AJSCCR

Keywords:

H2 production; Light irradiation; CuS/C3N4 nanocomposites; Photocatalyst

Citation:

Sponza DT. H2 Generation via CuS/C3N4 Nanocatalyst under Solar Light from the Municipale Wastewaters. Ame J Surg Clin Case Rep. 2022; 5(6): 1-7

1. Abstract

Hydrogen production via photocatalysis was very effective for sustainable green energy. CuS/C3N4 nanocatalysts were developed under laboratory conditions. XRD analysis showed that CuS with a hexagonal shape was produced and doped on the C3N4. TEM images results showed that CuS nanocatalysts were dispersed on the surface of C3N4 exhibiting a spherical type. The photocatalytic yield of the CuS/C3N4 nanocomposite produced under laboratory conditions was evaluated in municipal wastewaters based on chemical oxygen demand (COD)l as electron donor as a scavenger for H2 production under solar light. The photocatalytic activity for H2 production was promoted by increasing CuS contents from 1% up to 12%. The maximum H2 gas productions was 99% at a CuS/C3N4 nanocatalyst concentration of 4 mgl at a CuS percentage of 12% after 60 minutes photooxidation at a COD concentration of 980 mg/l. With the increase the loading of CuS percentage to 12% the produced nanocomposite indicated stability through visible light irradiation.

2. Introduction

Solar photocatalysis is a favorable technology for environmental treatment and energy production [1]. In particular, the H2 production reaction using semiconductors materials with various sacrifcial electron donors such as alcohols and carbohydrates in the presence of visible light illumination has been realized the main renewable source for clean energy [2]. Carbon nitride (C3N4) is a semiconductor with suitable applications such as energy, catalytic, and electronic [3]. C3N4 is cost-efective and effective photocatalyst under sunlight for H2 energy production with high redox reaction and suitable bandgap and OH productions [4]. C3N4-based photocatalysts could be formed at various nanostructures morphological depending on diferent preparation procedures such as nanorods, nanotubes, nanosheets, nanospheres, and others [5]. In general, two-dimensional (2D) g-C3N4 nanosheets have paid comprehensive attention for their exclusively electronic, optical, photoresponse abilities and biocompatible features compared with the bulk C3N4 [4, 5], which is explained by its unique 2D architecture, excellent chemical stability, environmentally benign characteristics, and harmonic electronic structure [6]. When the particle size is small, the space between the nanoparticles surface could be reduced the photogenerated electrons that restrain the recombination of electrons and holes. To enhance the performance.

Metal sulfde has received attention as heterogeneous semiconductor photocatalysts with interesting structure owing to their high photocatalytic performances in diferent potential applications such as photodegradation of toxic organic compounds [7]. Among metal sulfde nanoparticles, CuS is well known as a p type semiconductor with narrow bandgap and has band absorption close to infrared zone [8] and possesses weak visible light and high nearby infrared zone refectance, which create it a favorable material for absorption of visible light. In addition, CuS as an efect photocatalyst has been drawn attention because of its attractive photocatalytic efciency for H2 production and degradation of antibiotics, dyes, and herbicides [9, 10]. The previous researches showed that with C3N4 using photocatalysts a novel CuS/C3N4 heteronanoparticle was generated to remove some organics ana pruduce H2 [11, 12].

In this study, photocatalytic H2 production was aimed by the utilization of CuS nanoparticles deposited onto the C3N4 sheet from municipale wastewaters. The crystal ana morphological properties

of CuS/C3N4 nanocomposite was investigated. The effects of nanocomposite doses and CuS percentages and photocatalytic duration on the photocatalytic H2 production was investigated.

3. Materials and Methods

3.1. Production of C3N4 under Laboratory Conditions

C3N4 was developed by calcinating of 5 g melamine for 3 h at 600 °C. To manufacture C3N4 nanosheets, 2 g bulk C3N4 was grinded in a mortar and calcinated for 2 h in air at 520 °C. Manufacture of CuS nanoparticles CuS was synthesized by the dissolution of 3 mmol (0.543 g) of copper acetate and 3 mmol (0.228 g) of thiourea in 40 mL H2O. Then, the resultant mixture was agitated for 2 h to obtain a complete homogenous precipitate. The produced suspension was then put in a Tefon-lined autoclave and maintained for 24 h at 140 °C in a hydrothermal container. The obtained black CuS precipitate was separated via fltration, washed with water many intervals to get rid of any contaminants, and fnally kept to dry for 12 h in a drier at 60 °C.

3.2. Establishment of CuS/C3N4 Nanocomposites

About 50 mL of H2O was utilized to disperse 0.5g of C3N4 nanosheets via ultrasonication for 30 min. After that, copper acetate (0.068 g) was introduced to the previous solution and the resultant mixture was agitated via a magnetic stirrer for 60 min. A solution of 40 mL of water-containing 0.074 g thiourea was mixed together with the previously prepared suspension and the produced mixture was agitated for 5 h by a magnetic stirrer. Finally, the resultant suspension was put in a Tefon-lined autoclave for 24 h at 140 °C. The product was separated via fltration, washed with bidistilled water many intervals to get rid of any contaminants, and then left to dry in a drier for 12 h at 80 °C. The resultant photocatalyst nanocomposites were nominated as 12 wt% CuS/g-C3N4. Diverse wt% of x CuS/g-C3N4 (x=1 ,4, 6, 8 wt%) were furnished utilizing an analogous technique through adjusting the quantity of both thiourea and copper acetate then, designated as 1, 4, 6, 8 and 12 wt% CuS/C3N4 nanocomposites, respectively.

3.3. Investigation of Physicochemical Properties of CuS/C3N4 Nanocomposites

To determine the crystalline phases, Bruker axis D8 with Cu Kα radiation (λ =1.540 Å) was employed X-ray Diffraction (XRD) of the prepared nanocomposites at room temperature. To investigate nanostructure morphology, sample dimensions, surface morphology, and Transmission Electron Microscopy (TEM), JEOL-JEM-1230 was used. To determine X-ray Photoelectron Spectroscopy (XPS) measurements, Thermo Scientifc K-ALPHA spectrometer was conducted.

3.4. Photocatalytic Activity CuS/C3N4 Nanocomposites

The photocatalytic activity for H2 production over the prepared nanocomposites was conducted in Pyrex photoreactor top window cell 250 mL in circulation system after Ar gas purging to drive out the dissolved oxygen in H2O for 10 min before staring the photocatalytic reaction. A Xenon arc lamp 500 W was employed and maintained vertically above the photoreactor and UV cutof flter (λ>420 nm) was used to utilize for visible light. 60 mg 12 wt% CuS/g-C3N4 nanocomposite was suspended in 200 mL 10 vol% glycerol aqueous solution with magnetic stirring.

3.5. H2 Gas Measuremts

H2 gas generated in the photocatalytic reactor was analyzed every 40 minutes to determine hydrogen yield by gas chromatograph (Agilent GC 7890A system).

3.6. COD Measurement

COD in the municipal wastewater was measured according to Standard Methods (2017) [13].

4. Results and Discussion

4.1. XRD Analysis Results

By doping of increasing percentages of CuS nanoparticles (1%(a) , 4%(b), 6%(c), 8%(d) and 12%(e)) to C3N4; the peaks of sole C3N4, CuS nanoparticles, and CuS/C3N4 nanocomposite were measured by XRD analyses (Figure 1). The main XRD peak of the obtained C3N4 nanoparticle is located at 29.9° (JCPDS 87-1526), evidencing 0.319 nm an interlayer distance with difraction plane indexed as (002). For pure CuS nanoparticles, the XRD diffraction peaks are located at 29.0°, 33,1°, 47,9°, 50.9°, and 57.4°, corresponding hexagonal CuS facets (101), (102), (111) (109), and (119) (JCPDS No. 06-0464) as reported by . The variations in XRD peaks of CuS nanoparticles in heterogen CuS/C3N4 nanocomposites showed that the CuS nanoparticles have been decorated the C3N4 nanosheets. The stronger XRD peaks of CuS nanoparticles in CuS/C3N4 were observed at 8% and 12 wt% CuS/C3N4 nanocomposites; while XRD peaks were not owing the low CuS dispersion onto C3N4 surface at low CuS contents like 1% and 4%.

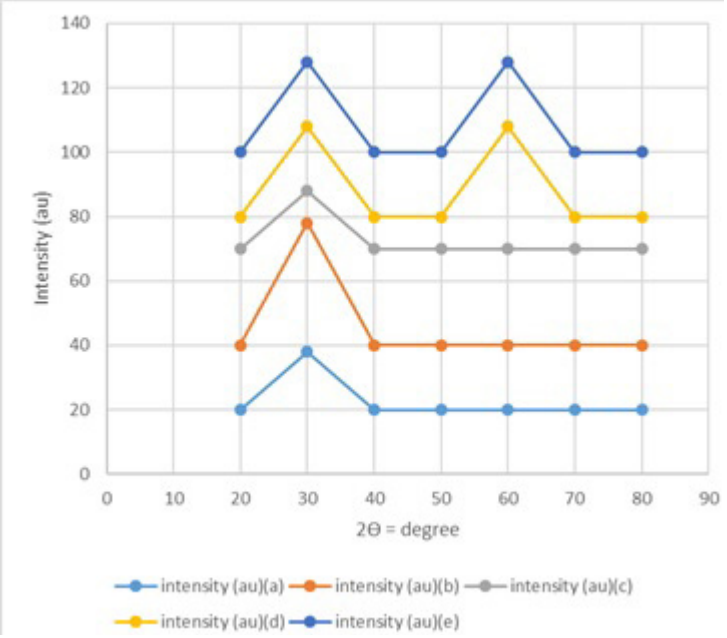

Figure 1: XRD analysis results of doped increasing percentages of CuS nanoparticles (1%(a) , 4%(b), 6%(c), 8%(d) and 12%(e)) to C3N4.

4.2. FTIR Analysis Results

Figure 2 exhibited the FTIR spectra of C3N4, 4% and 12 wt% CuS/C3N4 nanosheets. The stretching scale was detected at 808 cm−1 peak corresponding triazine units in pure C3N4 nanosheets. However, there is alow shift at 808 cm−1 for 4% and 12 wt% CuS/C3N4 nanocomposite, shifting an effective coupling between CuS nanoparticles and C3N4. It was shown that FTIR peak intensity decreased with the increase of CuS percentage. There are fve peaks exhibited at 1250 cm−1, 1325 cm−1, 1439 cm−1, 1575 cm−1, and 1639 cm−1 produced after CN—spreading step [14, 15]. A different peak in the range of 3600–3000 cm−1 was detected. This can be defined as result of NH-spreading oscillation. These peaks are not shifted after CuS nanoparticle doping to C3N4.

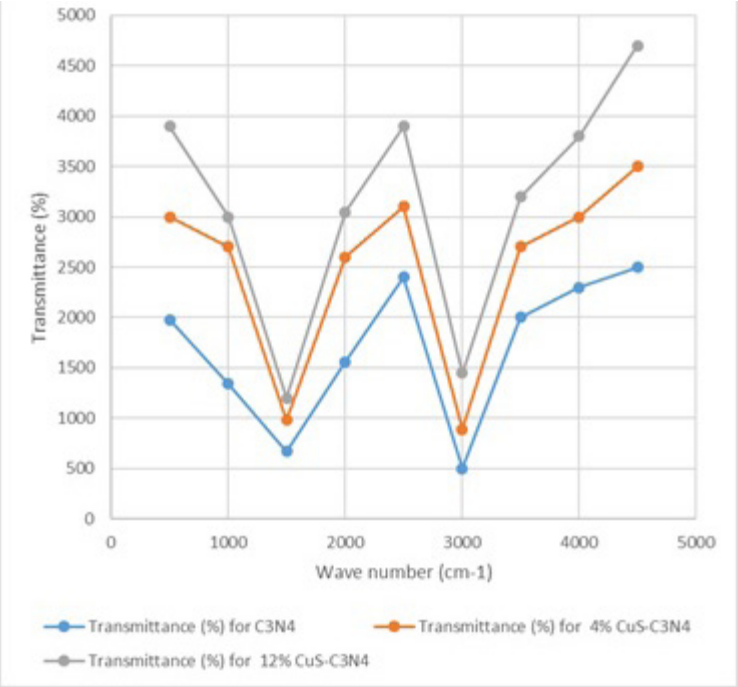

Figure 2: FITR analysis results of XPS spectra analysis

4.3. XPS Spectra Analysis

The chemical valence state and bond configuration of novel C3N4/CuS heterojunctions was analyzed by X-ray photoelectron spectrum. As shown in Figure 3a, the survey spectrum, C, N, S, Cu and O were detected in the sample of C3N4/CuS-2, and the O on the surface of the C3N4/CuS-2 was came from the adsorption of oxygen from the atmosphere. Besides, the Cu, S and N were only detected in the spectra of g-C3N4 and CuS, respectively. These results were well in accordance with the chemical composition of the as-prepared sample, which also confirmed by the XRD and FTIR analysis. The high resolution X-ray photoelectron spectra of C 1s were shown in Figure 3b. CuS showed only one peak at 284.8 eV, which could be assigned to the external hydrocarbon contamination. While in the spectra of C3N4 and C3N4/CuS-2 had the other peak at around 288.2 eV and 288.6 eV were came from the N-C=N in its chemical bone structure, which indicated the existence of g-C3N4. Besides, the C 1s binding energy of C3N4/CuS-2 was slightly higher than that of g-C3N4. In the N 1s high resolution XPS spectra of g-C3N4, several peak at 398.8 eV, 399.8 eV, 400.9 eV and 404.6 eV which could be ascribed to N (C-N=C) groups (sp2 bonded), tertiary nitrogen N-(C)3 groups, C-N-H amino groups and the charging effects, respectively [17, 18]. Notably, the N 1s binding energy of g-C3N4/CuS-2 was slightly higher than that of g-C3N4, which is similar to the C 1s peak of N-C=N groups at 288.3 eV. Meanwhile, combined with the slight shift in the C 1s and N 1s spectra, the result represented the interactions between CuS and g-C3N4 (x), which may be the chemical bonds of Cu-S-N or Cu-S-C. In comparison, the Cu 2p3/2 and Cu 2p1/2 peaks of CuS appeared at 932.8 eV and 952.7 eV, respectively, which were highly than the corresponding binding energy of g-C3N4/CuS-2 at 932.1 eV and 952.0 eV, respectively (Figure 3c).

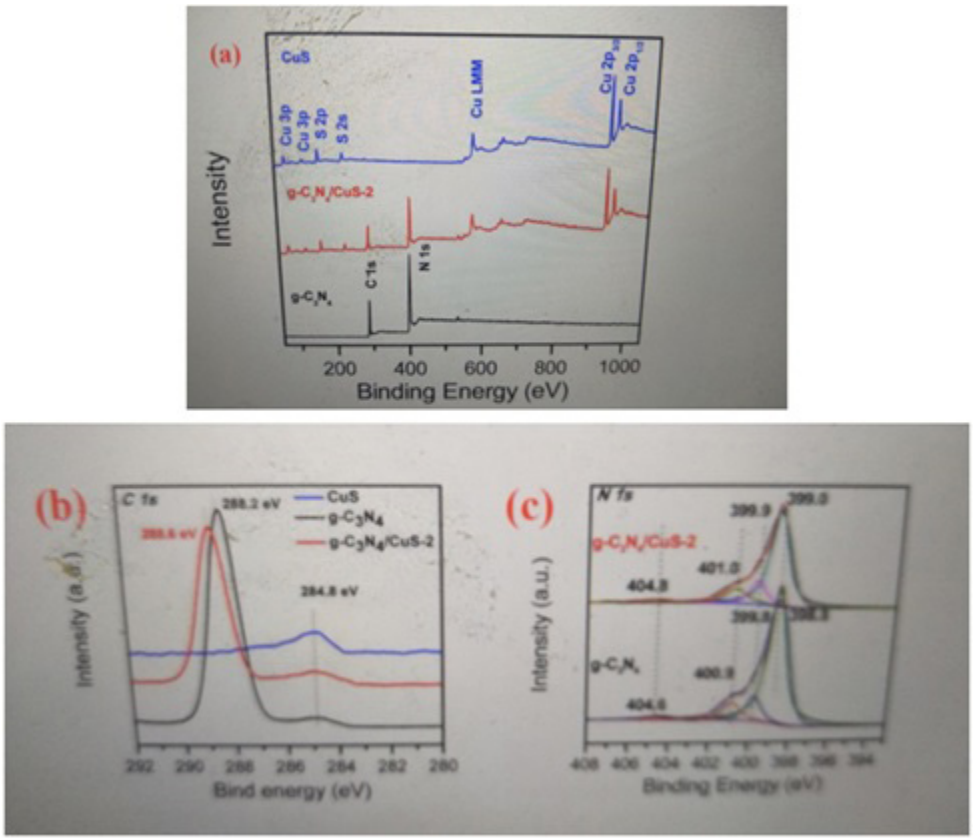

Figure 3: XPS analysis results of C3N4/CuS heteronanocomposite

4.4. Temanalysis Results

The typical TEM image (Figure 4a) of C3N4 shows 2D sheet-like nanostructures with transparent thin layers resembling the graphene nanosheets. For CuS sample (Figure 4b), irregularly aggregation can be observed. However, surprisingly, by the hydrothermal method to prepare C3N4/CuS nanocomposite, the TEM result (Figure 4c) clearly confrmed the successful loading of CuS NPs onto the C3N4 nanosheet surface, and no free CuS NPs were present in the suspension [19]. A higher magnication TEM image (Figure 4d) clearly demonstrate that the average size of CuS NPs is around 11.0 nm (data not shown).

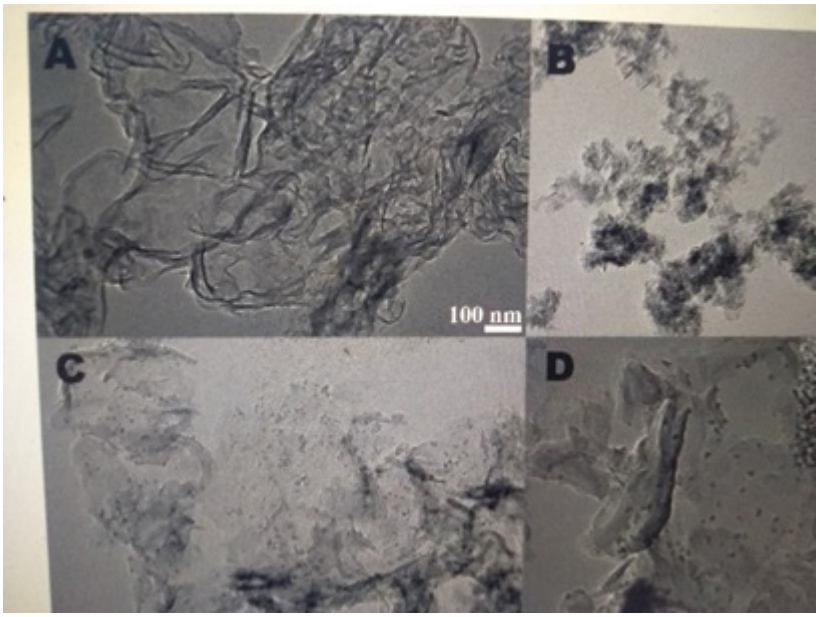

Figure 4: TEM images of C3N4 (a) for CuS (b) C3N4/CuS nanocomposite,(c) ana loading of CuS to CEN4/CuS nanoparticle.

4.5. HRTEM Analysis Results

The HRTEM images in Figure 5e shows that the lattice fringes with dispacing of 0.31 nm can be assigned to the (102) crystal plane of hexagonal CuS phase. These results indicate that the C3N4 nanosheets signifcantly infuence the growth of CuS NPs and effectively restrain their aggregations [20]. It could be attributed to two possible reasons. First, the C3N4 nanosheet may act as a two-dimensional "mat" that interacts with CuS NPs through physisorption to hinder their aggregation [20]. Second, the oxygen-containing defects and the amino groups on g-C3N4 surface could serve as anchor sites to immobilization of the N, Cu and S. (Figure 5f).

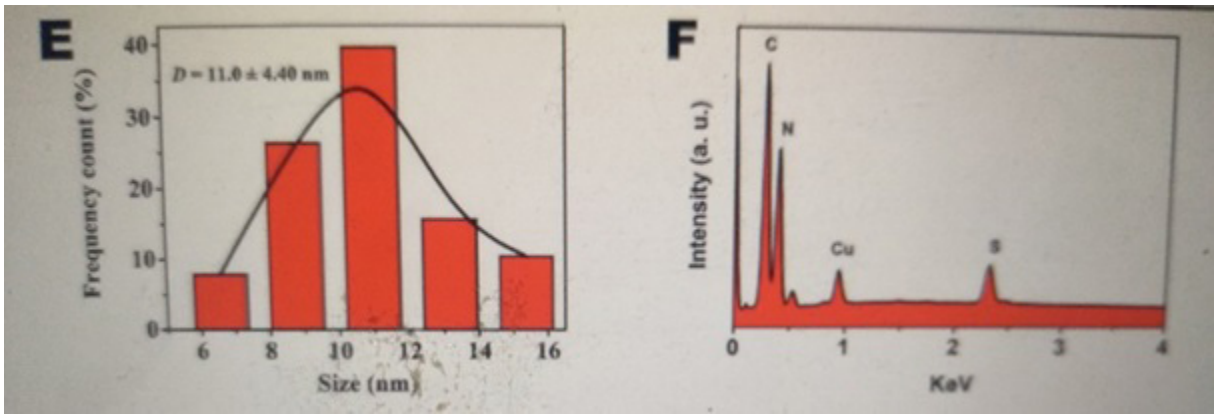

Figure 5: HRTEM images of hexagonal CuS phase with size ditributions a),the molecular composition of the C3N4-CuS nanocomposite.

4.6. H2 Productıon

The photocatalytic activity of the C3N4/CuS composite was assessed by the photodegradation of amunicipal wastewater containing glucose under visible light (l > 420 nm) irradiation with a COD concentaton of 890 mg/l (Figure 6). Municipal wastewater was used as a target pollutant to evaluate the photocatalytic activity of the as-prepared samples because the photodegradation of municipal is negligible under visible light, confirming that the photocatalytic activity indeed originates from the photocatalyst. Prior to irradiation, the suspensions were magnetically stirred in dark for 20 min to obtain the absorption–desorption equilibrium between the photocatalysts and COD. The variation in the absorption intensity of COD solution over CuS, C3N4, and C3N4/x wt% CuS (x 1 wt%, 4 wt%,6 wt%, and 12 wt%) at different irradiation were investigated. As shown in Fig. 6, 890 mg/l COD are photodegraded by CuS and pure C3N4, respectively. While the C3N4/CuS composite have a CuS percentage of 12% the highest photodegradation ratio and H2 gas production was detected after 60 min. Approximately 96% of COD was decomposed. Furthermore, as the CuS content in the composites decreases, the photocatalytic activity of the composite starts to decrease. CuS doesn't show any visible light activity in the photocatalytic degradation of COD. To be served as a good photocatalyst, except for the enhanced visible light activity, the reusability and stability are also extremely important [21, 22].

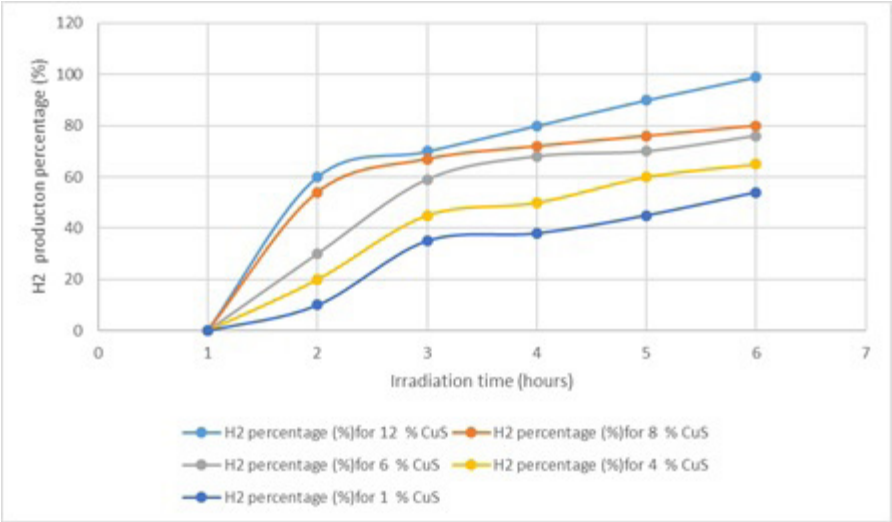

Figure 6: H2 production percentage versus CuS percentages in the C3N4/CuS nanocomposite.

4.7. Effect of Increasing C3N4/CuS Nanocomposite doses with a CuS Percentage of 12% on the H2 Production Rates

As the C3N4/CuS nanocomposite concentrations were increased from 0,5 mg/l to 2, 3 and 4 mg/l the H2 production percentage increased from 23% up to 99% (Table 1). Further incease of the nanocomposite dose up to 6 and 8 mg/l a significant H2 production was not detected. The optimal C3N4/CuS nanocomposite dose from maximum H2 production percentage of 99% was detected at a nanocomposite dose of 4 mg/l with a CuS percentage of 12%.

Table 1: Effect of increasing C3N4/CuS nanocomposite doses on the H2 production percentage.

C3N4/CuS nanocomposite concentrations(mg/l)	0,5	1	2	3	4	6	8
H2 production percentage (%)	23	60	72	80	99	98	98

5. Conclusions

In conclusion, the novel porous g-C3N4/CuS nanocomposites were successfully prepared under laboratoy conditions. By introduction of C3N4, of CuS the surface of g-C3N4 was homogenous distributed and avoid severe agglomeration. The enhanced photocatalytic activity of the C3N4/CuS could be ascribed to the formation of a heterojunction, which improved the efficient transfer of photoinduced electron-holes between the interface of C3N4 and CuS to produce H2.

References

1. Chen CC, Ma WH, Zhao JC. Semiconductor-mediated photodegradation of pollutants under visible-light irradiation, Chem. Soc. Rev. 2010; 39: 4206-19.
2. Linsebigler AL, Lu GQ, JTY Jr. Photocatalysis on TiO2 Surfaces: Principles, Mechanisms, and Selected Results, Chem. Rev. 1995; 95: 735-758.
3. Huang ZA, Sun Q, Lv KL, Xhang ZH, Li M, Li B. Effect of contact interface between TiO2 and g-C3N4 on the photoreactivity of g-C3N4/TiO2 photocatalyst: (001) vs (101) facets of TiO2, Appl. Catal. B: Environ. 2015; 164: 420-7.
4. Pan J, Li TJ, Yan ZL, Zhou BH, Wu HS. SnO2@CdS nanowire-quantum dots heterostructures: tailoring optical properties of SnO2 for enhanced photodetection and photocatalysis, Nanoscale. 2013; 5: 3022-9.
5. Hu SZ, Ma L, You JG, Li FY, Fan ZP, Lu G, et al. Enhanced visible light photocatalytic performance of g-C3N4 photocatalysts co-doped with iron and phosphorus, Appl. Surf. Sci. 2014; 311: 164-71.
6. Wang YG, Wang YZ, Chen YT, Yin CC, Zou YH, Cui LF. Synthesis of Ti-doped graphitic carbon nitride with improved photocatalytic activity under visible light, Mater. Lett. 2015; 139: 70-2.
7. Samanta S, Martha S, Parida K. Facile Synthesis of Au/g-C3N4 Nanocomposites: An Inorganic/Organic Hybrid Plasmonic Photocatalyst with Enhanced Hydrogen Gas Evolution under Visible-Light Irradiation, ChemCatChem. 2014; 5: 1453-62.
8. Xue JJ, Ma SS, Zhou YM, Zhang ZW, He M. Facile Photochemical Synthesis of Au/Pt/g C3N4 with Plasmon-Enhanced Photocatalytic Activity for Antibiotic Degradation, ACS Appl. Mater. Inter. 2015; 7: 9630-7.
9. Zheng Y, Liu J, Liang J, Jaroniee M, Qiao SZ. Graphitic carbon nitride materials: controllable synthesis and applications in fuel cells and photocatalysis, Energy Environ. Sci. 2012; 5: 6717-31.
10. Naseri A, Samadi M, Pourjavadi AZ, et al. Graphitic carbon nitride (g-C3N4)-based photocatalysts for solar hydrogen generation: recent advances and future development directions[J]. J Mater Chem A. 2017; 5: 23406-33.
11. Wang XC, Maeda K, Thomas A, et al. A metalfree polymeric photocatalyst for hydrogen production from water under visible light[J]. Nat Mater. 2009.
12. Liu JH, Zhang T, Wang ZG, et al. Simple pyrolysis of urea into graphitic carbon nitride with recyclable adsorption and photocatalytic activity[J]. J Mater Chem. 2011; 21: 14398-401.
13. Standard Methods for examination of water ana wastewater, APHA-AWWA, USA, 2017.
14. Wang XC, Blechert S, Antonietti M. Polymeric graphitic carbon nitride for heterogeneous photocatalysis[J]. ACS Catal. 2012; 2(8): 1596-606.
15. Cheng NY, Tian JQ, Liu Q, et al. Aunanoparticle-loaded graphitic carbon nitride nanosheets: Green photocatalytic synthesis and application toward the degradation of organic pollutants[J]. ACS Appl. Mater. Interfaces. 2013; 5(15): 6815-9.
16. Ong WJ, Tan LL, Ng YH, et al. Graphitic carbon nitride(g-C3N4)-based photocatalysts for artificial photosynthesis and environmental remediation: Are we a step closer to achieving sustainability?]. Chem Rev. 2016; 116: 7159-329.
17. Di Y, Wang XC, Thomas A, et al. Making metalcarbon nitride heterojunctions for improved photocatalytic hydrogen evolution with visible light[J]. ChemCatChem. 2010; 2(7): 834-8.
18. Bhunia K, Chandra M, Khilari S, et al. Bimetallic PtAu alloy nanopartices-intergrated g-C3N4 as an efficient photocatalyst for water-to-hydrogen conversion[J]. ACS Applied Materials & Interfaces, 2018.
19. Chen S, Wang C, Bunes BR, et al. Enhancement of visible-light-driven photocatalytic H2 evolution from water over g-C3N4 through combination with perylene diimide aggregates [J]. Applied Catalysis A: General. 2015; 498: 63-8.
20. Qin J, Huo J, Zhang P, Zeng J, et al. Improving the photocatalytic hydrogen production of Ag/gC3N4 nanocomposites by dye-sensitization under visible irradiation[J]. Nanoscale. 2016; 8(4): 2249-59.

21. Liu Y, Wu X, Lv H, et al. Boosting the photocatalytic hydrogen evolution activity of gC3N4 nanosheets by Cu2(OH)2CO3 modification and dye-sensitization[J]. Dalton Trans. 2019; 48: 1217-25.
22. Paul T, Das D, Das BK, et al. CsPbBrCl2/gC3N4 type II heterojunction as efficient visible range photocatalyst [J]. Journal of Hazardous Materials. 2019; 380: 120855.
23. Yang LY, Liu J, Yang LP, et al. Co3O4 imbedded g-C3N4 heterojunction photocatalysts for visiblelight-driven hydrogen evolution [J]. Renewable Energy. 2020; 145: 691-8.